ChemComm

COMMUNICATION

View Article Online
View Journal | View Issue

Cite this: *Chem. Commun.*, 2018, **54**, 12762

Received 1st October 2018,
Accepted 18th October 2018

DOI: 10.1039/c8cc07858k

rsc.li/chemcomm

An oxaliplatin(IV) prodrug-based supramolecular self-delivery nanocarrier for targeted colorectal cancer treatment†

Wei Qi Lim,[ab] Soo Zeng Fiona Phua,[b] Hongzhong Chen[b] and Yanli Zhao *[b]

A redox-responsive supramolecular nanocarrier was constructed from the self-assembly of spermine modified cyclodextrin and oxaliplatin prodrug. The nanocarrier could preferentially accumulate in polyamine transporter over-expressing HCT116 cells, releasing drugs under a reducing intracellular environment to maximize anti-cancer treatment.

Platinum-based anticancer drugs are among the most widely used chemotherapeutics for the treatment of colorectal cancer. Despite their success, these drugs often suffer from some drawbacks such as poor tumor selectivity and accumulation as well as dosage-dependent drug resistance, thus limiting their applications to some extent.[1] To address these problems, considerable research progress had been made to develop sophisticated drug carriers for targeted delivery to tumors.[2] However, the low drug loading capacity, potential systemic toxicity, complex fabrication, and related metabolism concern of these multifunctional nanocarriers have hampered their clinical translations toward practical uses.[3]

Carrier-free Pt(IV) prodrug delivery systems are a novel kind of therapeutics.[4] Such prodrugs are easily prepared by introducing two axial ligands to a Pt(II) drug to not only tune the redox potential of the platinum core to Pt(IV) but also change the hydrophobicity/hydrophilicity balance.[5] The amphiphilic molecular prodrugs could in turn form nanostructures that act as both carriers and cargoes.[6] Compared to traditional carrier-based drug delivery systems, such carrier-free self-delivery nanosystems demonstrate much higher drug loading capacity and eliminate the toxicity concerns of the drug carriers, whilst having the nanoscale advantage of the enhanced permeability and retention (EPR) effect to achieve passive accumulation at the tumor site.[7] To become pharmacologically active, Pt(IV) prodrugs need to undergo intracellular reduction discriminatingly in cancer cells containing high concentrations of endogenous reducing agents.[8] This feature could reduce side effects to normal cells, as the activation of the active drug is selective in cancer cells.

In this work, we report the fabrication of self-assembled nanoparticles through the host–guest complexation between spermine-functionalized β-cyclodextrin (CD-spermine) and cholesterol-conjugated oxaliplatin(IV) (oxliPt(IV)-chol) for colorectal cancer-targeted and redox-responsive drug delivery (Scheme 1). Each component in the nanocarrier had an irreplaceable function, *i.e.*, oxaliplatin(IV) as a prodrug, spermine as a targeting ligand, and cholesterol and β-cyclodextrin for the formation of an inclusion complex with inherent amphiphilicity for the self-assembly.[9] As a natural biomolecule involved in cellular biochemical pathways such as signalling and protein biosynthesis, polyamine spermine exhibits favourable biocompatibility and minimal side effects.[10] Colorectal cancer cells were found to overexpress polyamine transportation receptors in order to scavenge polyamines from exogenous sources for sustaining rapid cell division.[11] Hence, spermine could function as an active targeting ligand

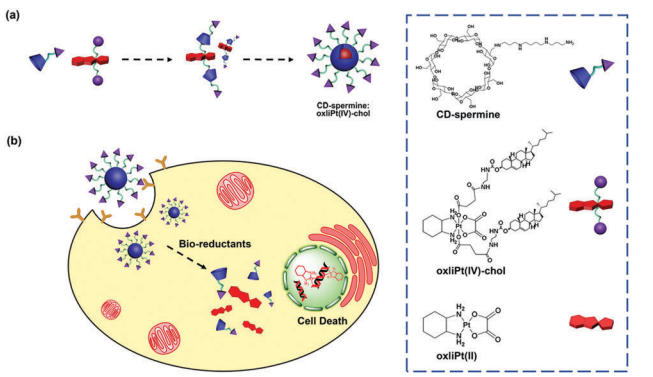

Scheme 1 Schematic illustration of (a) self-assembly of CD-spermine and oxliPt(IV)-chol for the formation of CD-spermine: oxliPt(IV)-chol nanoparticles and (b) redox-responsive drug release in cancer cells.

[a] *NTU-Northwestern Institute for Nanomedicine, Interdisciplinary Graduate School, Nanyang Technological University, Singapore*
[b] *Division of Chemistry and Biological Chemistry, School of Physical and Mathematical Sciences, Nanyang Technological University, 21 Nanyang Link, Singapore 637371. E-mail: zhaoyanli@ntu.edu.sg*

† Electronic supplementary information (ESI) available: Synthesis and characterization details. See DOI: 10.1039/c8cc07858k

for enhanced accumulation of the nanocarrier in colorectal cancer cells.

The oxliPt(IV)-chol prodrug as a guest molecule was prepared by reacting ethylenediamine-modified cholesterol with oxliPt(IV)–COOH (Schemes S1 and S2, ESI†). The chemical structures of the intermediates and final product were fully characterized *via* several analytical techniques (Fig. S1 and S2, ESI†). CD-spermine as the host molecule was attained by reacting excess spermine with tosylated β-cyclodextrin (Scheme S3, ESI†). Its structure was well characterized with ^{1}H NMR and mass spectrometry. A decrease in the zeta potential from −20.1 mV of β-cyclodextrin to −6.8 mV of CD-spermine also indicated the successful synthesis of CD-spermine (Fig. S3, ESI†). Such changes could be attributed to the reduction of the anionic hydroxyl groups on β-cyclodextrin after the conjugation with spermine that carries highly positive amino units.

Before preparing the self-assembled nanoparticles, we investigated whether the molecular prodrug could undergo the reduction to give active oxaliplatin(II) species. High-performance liquid chromatography (HPLC) and liquid chromatography-mass spectrometry (LC-MS) were employed to study the reduction reaction products of oxliPt(IV)-chol incubated with sodium ascorbate. The reduction of the prodrug was expected to lead to the dissociation of the axial cholesterol ligand and produce active oxaliplatin (Fig. S4, ESI†). HPLC monitoring revealed that the reaction outcome was indeed consistent with our expectation. A peak corresponding to oxliPt(IV)-chol (retention time: 17 min) disappeared after the reduction with sodium ascorbate, whilst there was an emergence of a new peak corresponding to oxliPt(II) (retention time: 9.5 min). In addition, the LC-MS spectrum of the reaction solution confirmed the presence of the active oxaliplatin drug and cholesterol ligand after the reduction reaction. These results indicate that our designed molecule could indeed function as a redox-responsive prodrug. It is pharmacologically inactive and requires reductive elimination to achieve the active form.

The cytotoxicity of oxaliplatin arises from the formation of an adduct with DNA nucleobases, specifically binding to the N7 guanine.[12] Hence, the ability of the released oxaliplatin drug binding with DNA was investigated. 5′-GMP was used to stimulate the interaction mechanism of the drugs with DNA, where the adduct products were studied by HPLC and LC-MS (Fig. S5, ESI†). Taking the result of the direct reaction of oxaliplatin(II) with 5′-GMP as the reference, HPLC peaks at the retention times of 8.4 min and 10.2 min were found, corresponding to the adduct of oxaliplatin(II) with one and two 5′-GMP, respectively. The same peaks appeared for the reaction between the reduced oxliPt(IV)-chol prodrug and 5′-GMP, indicating that the released platinum species from the prodrug was most likely oxaliplatin(II) and could possibly exhibit similar behavior *in vitro*.

To prepare CD-spermine: oxliPt(IV)-chol nanoparticles, we first quantitatively investigated the binding stoichiometry between CD-spermine and oxliPt(IV)-chol. A Job's plot was obtained to determine the host–guest inclusion ratio of 2 : 1 (Fig. 1a). ^{1}H NMR spectra of CD-spermine revealed changes in the chemical shifts of characteristic protons before and after binding with 0.5 equivalent of oxliPt(IV)-chol, attributing to the complexation-induced shielding

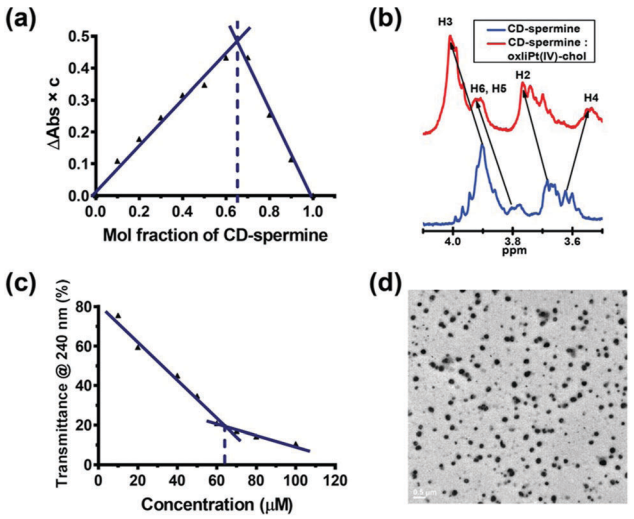

Fig. 1 (a) Job's plot indicating a 2 : 1 binding ratio between CD-spermine and oxliPt(IV)-chol, (b) ^{1}H NMR comparison of CD-spermine and CD-spermine: oxliPt(IV)-chol complex in D_2O/DMSO-d_6 (5/5, v/v), (c) plot of concentration-dependent optical transmittance changes of oxliPt(IV)-chol at 240 nm in the nanoparticle formation, and (d) TEM image of CD-spermine: oxliPt(IV)-chol nanoparticles.

effect (Fig. 1b). This result demonstrated that the cholesterol moiety of the prodrug was included into the hydrophobic cavity of the cyclodextrin host to form a supramolecular complex. Based on the obtained binding ratio, CD-spermine: oxliPt(IV)-chol nanoparticles were prepared by mixing oxliPt(IV)-chol in DMSO with CD-spermine aqueous solution. The critical aggregation concentration (CAC) of the complex was determined to be 64.9 μM by monitoring the change in the optical transmittance at 240 nm upon increasing the concentration of oxliPt(IV)-chol (Fig. 1c). The as-prepared CD-spermine: oxliPt(IV)-chol nanoparticles were then characterized *via* transmission electron microscopy (TEM), and the obtained images revealed a well-dispersed spherical morphology (Fig. 1d). The nanoparticles exhibited a narrow size distribution with an average hydrodynamic diameter of 130 nm as measured by dynamic light scattering (Fig. S6, ESI†). The oxaliplatin encapsulation efficiency was 22.7 wt% as measured by inductively coupled plasma-optical emission spectrometry (ICP-OES).

To evaluate the redox-triggered drug release properties of the CD-spermine: oxliPt(IV)-chol nanoparticles, the cumulative drug release of Pt from the nanoparticles was studied using ICP-MS (Fig. 2). 5 mM sodium ascorbate solution was used to simulate the reducing environment inside cancer cells.[13] In the absence of sodium ascorbate, there was only around 25% Pt detected after 24 h, suggesting that the nanoparticles were relatively stable under physiological conditions. In comparison, in 5 mM sodium ascorbate, the released amount of Pt drastically increased to 63%, illustrating that the CD-spermine: oxliPt(IV)-chol nanoparticles could be an effective drug delivery system. The encapsulated Pt(IV) prodrug would only be released in the presence of enough amount of reducing agents in the intercellular matrix of cancer cells. This feature ensured minimal drug leakage before the cellular uptake for reduced side effects.

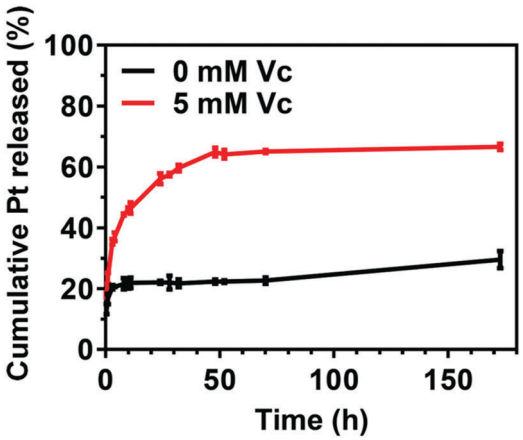

Fig. 2 Cumulative platinum drug release profile from CD-spermine: oxliPt(IV)-chol nanoparticles in PBS solution (pH 7.4) and in 5 mM sodium ascorbate solution.

The cellular uptake of CD-spermine: oxliPt(IV)-chol nanoparticles was evaluated using fluorescein isothiocyanate (FITC)-labelled nanoparticles. Fig. 3a shows the confocal laser scanning microscopy (CLSM) images of colorectal cancer HCT116 cells after the incubation with the nanoparticles at 2 h and 18 h. After 2 h of incubation, a little green fluorescence was observed inside the cells, implying that the nanoparticles hardly entered the cells. On the other hand, the enhanced cellular FITC fluorescence after 18 h of incubation was evident that the CD-spermine: oxliPt(IV)-chol nanoparticles could be internalized with time. Flow cytometry also confirmed that the uptake of the nanoparticles was time-dependent (Fig. S7, ESI†).

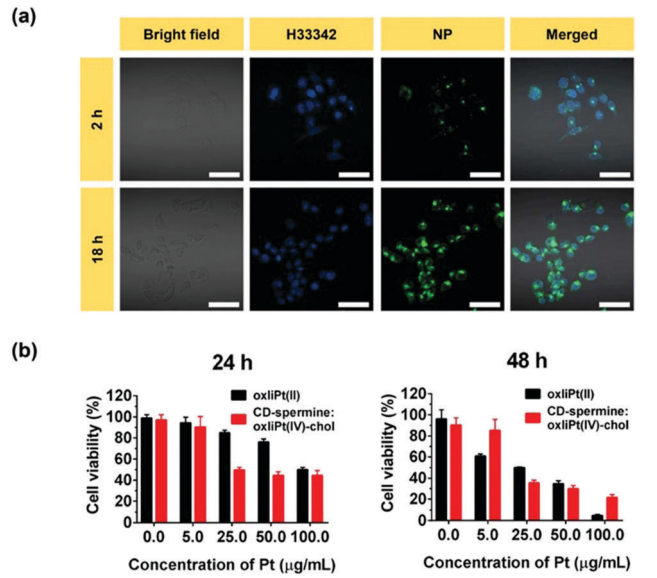

Fig. 3 (a) CLSM images of HCT116 cells incubated with FITC-labelled CD-spermine: oxliPt(IV)-chol nanoparticles. Cell nuclei were stained by H33342. Scale bar: 50 μm. (b) *In vitro* cytotoxicity of oxliPt(II) and CD-spermine: oxliPt(IV)-chol nanoparticles incubated with HCT116 cells for 24 and 48 h.

Subsequently, the anticancer efficacy of the nanoparticles was evaluated *via* 3-(4,5-dimethylthiazol-2-yl)-2,5-diphenyltetrazolium bromide (MTT) assay. The cytotoxicity of CD-spermine alone on HCT116 cells was first evaluated and the obtained results showed low cytotoxicity. Hence, CD-spermine would have a minimal effect on the cytotoxicity of the nanocarrier system (Fig. S8, ESI†). Then, oxliPt(II) and CD-spermine: oxliPt(IV)-chol nanoparticles with various Pt concentrations from 1 to 100 μM were incubated with HCT116 cells for 24 h and 48 h. As shown in Fig. 3b, the CD-spermine: oxliPt(IV)-chol nanoparticles exhibited both concentration- and time-dependent cytotoxicity. The nanoparticles presented higher cytotoxicity to HCT116 cells as compared to free oxliPt(II) possibly due to enhanced cellular accumulation of the nanoparticles. The internalization of the drug-containing nanoparticles *via* the transporter-mediated process is more efficient than simple molecular diffusion of the free platinum drug within the same incubation time. Thereby, a better cell killing effect was observed for the nanoparticles. ICP-MS results of the cellular Pt uptake showed that the accumulation of CD-spermine: oxliPt(IV)-chol nanoparticles was about 30-fold greater than that of oxliPt(II) at 12 h incubation (Fig. S9, ESI†), verifying that the enhanced endocytosis of the nanoparticles was due to its nanosize and targeting effect of spermine. At a longer incubation time, however, the therapeutics effect of CD-spermine: oxliPt(IV)-chol nanoparticles (IC_{50} = 41.2 μM at 48 h) was not significantly better than that of the free oxaliplatin (IC_{50} = 37.7 μM at 48 h). This observation might be the result of the time-dependent drug release characteristics of the nanoparticles. Despite the enhanced cellular uptake, the nanoparticles had to undergo the reduction of the Pt(IV) species to its active Pt(II) form and subsequent dissociation and diffusion from the nanoparticles before inhibiting the cell growth. Moreover, it was plausible that not all of oxliPt(IV)-chol prodrug was reduced under these conditions, offsetting the effect of increased nanoparticle accumulation and mitigating the corresponding cytotoxicity *in vitro*.

To confirm the targeting ability of the spermine ligand, FITC labelled CD-NH_2: oxliPt(IV)-chol nanoparticles as a control group were also prepared for comparison. It was anticipated that the cellular uptake of these nanoparticles would be lower as the ethylenediamine ligand of CD-NH_2 cannot be recognized by the polyamine transporter, thereby reducing the rate of cellular internalization. As shown in Fig. S10, ESI,† the fluorescence intensity of FITC was stronger in the CLSM images of the CD-spermine: oxliPt(IV)-chol treated cells than those treated with the control nanoparticles, indicating that the spermine modification could promote cellular uptake probably through the transporter-mediated pathway. Furthermore, the HCT116 cell viability after incubating with CD-spermine: oxliPt(IV)-chol nanoparticles at 24 h and 48 h was shown to be lower than that of CD-NH_2: oxliPt(IV)-chol nanoparticles (Fig. 4a). The higher cytotoxicity of the CD-spermine: oxliPt(IV)-chol nanoparticles could be due to their increased cellular uptake *via* polyamine transporter-mediated endocytosis. In addition, competitive inhibition of the polyamine transporter was carried out by pretreating cells with spermine prior to the incubation with CD-spermine: oxliPt(IV)-chol nanoparticles. As observed in Fig. 4b and c, the fluorescence

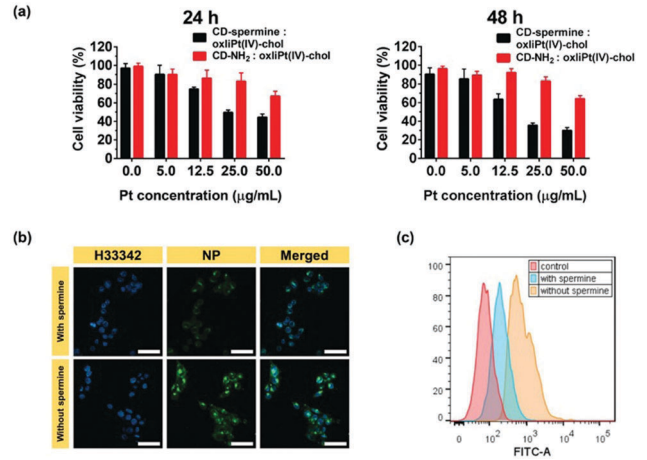

Fig. 4 (a) *In vitro* cytotoxicity of CD-spermine: oxliPt(IV)-chol and CD-NH_2: oxliPt(IV)-chol nanoparticles incubated with HCT116 colorectal cancer cells for 24 h and 48 h. Competitive intracellular uptake of CD-spermine: oxliPt(IV)-chol nanoparticles by spermine: (b) CLSM images and (c) flow cytometry profiles of HCT116 cells without and with pre-treatment of spermine prior to the incubation with FITC-labelled CD-spermine: oxliPt(IV)-chol nanoparticles. Cell nuclei were stained by H33342. Scale bar: 50 μm.

intensity of cells incubated with FITC labelled CD-spermine: oxliPt(IV)-chol nanoparticles was significantly higher than that of the spermine-pretreated group, once again demonstrating that the uptake of the nanoparticles was closely related to the polyamine transporter.

In summary, redox-responsive supramolecular prodrug nanoparticles have been successfully constructed *via* host–guest interaction. OxliPt(IV)-chol and CD-spermine not only serve as the building units, but also as the cargo and an active targeting component, respectively. Thus, the supramolecular nanoparticles prepared using this unique strategy integrate the advantages of active targeting, prodrug, and carrier-free systems, while simplifying the assembly complexity. The prodrug could be released under a reductive cellular microenvironment, allowing for controlled drug release. Importantly, *in vitro* experiments have confirmed that the CD-spermine: oxliPt(IV)-chol nanoparticles offered comparable cytotoxicity as free platinum drugs and provided specificity to cancer cells based on their redox responsiveness and targeting capability. This work presents an alternative strategy to the development of smart supramolecular nanocarriers, showing great potential in the field of controlled drug release and delivery toward cancer treatment.

This research was supported by the Singapore Academic Research Fund (No. RG11/17 and RG114/17) and the Singapore National Research Foundation Investigatorship (No. NRF-NRFI2018-03).

Conflicts of interest

There are no conflicts to declare.

Notes and references

1 (*a*) D. M. Kweekel, H. Gelderblom and H. J. Guchelaar, *Cancer Treat. Rev.*, 2005, **31**, 90–105; (*b*) T. Alcindor and N. Beauger, *Curr. Oncol.*, 2011, **18**, 18–25.
2 (*a*) J. Della Rocca, R. C. Huxford, E. Comstock-Duggan and W. Lin, *Angew. Chem., Int. Ed.*, 2011, **50**, 10330–10334; (*b*) Y. R. Zheng, K. Suntharalingam, T. C. Johnstone and S. J. Lippard, *Chem. Sci.*, 2015, **6**, 1189–1193; (*c*) J. Xu, Y. Kuang, R. Lv, P. Yang, C. Li, H. Bi, B. Liu, D. Yang, Y. Dai, S. Gai, F. He, B. Xing and J. Lin, *Biomaterials*, 2017, **130**, 42–55.
3 P. Ma, H. Xiao, C. Li, Y. Dai, Z. Cheng, Z. Hou and J. Lin, *Mater. Today Chem.*, 2015, **18**, 554–564.
4 (*a*) Z. Guo, Y. Zou, H. He, J. Rao, S. Ji, X. Cui, H. Ke, Y. Deng, H. Yang, C. Chen, Y. Zhao and H. Chen, *Adv. Mater.*, 2016, **28**, 10155–10164; (*b*) Y. Yuan, C.-J. Zhang and B. Liu, *Chem. Commun.*, 2015, **51**, 8626–8629; (*c*) S. He, C. Li, Q. Zhang, J. Ding, X.-J. Liang, X. Chen, H. Xiao, X. Chen, D. Zhou and Y. Huang, *ACS Nano*, 2018, **12**, 7272–7281.
5 (*a*) J. J. Wilson and S. J. Lippard, *Chem. Rev.*, 2014, **114**, 4470–4495; (*b*) M. D. Hall and T. W. Hambley, *Coord. Chem. Rev.*, 2002, **232**, 49–67; (*c*) T. C. Johnstone, K. Suntharalingam and S. J. Lippard, *Chem. Rev.*, 2016, **116**, 3436–3486.
6 (*a*) A. G. Cheetham, R. W. Chakroun, W. Ma and H. Cui, *Chem. Soc. Rev.*, 2017, **46**, 6638–6663; (*b*) C. Wang, Z. Wang and X. Zhang, *Acc. Chem. Res.*, 2012, **45**, 608–618.
7 (*a*) J. Zhou, G. Yu and F. Huang, *Chem. Soc. Rev.*, 2017, **46**, 7021–7053; (*b*) G. Yu, X. Zhao, J. Zhou, Z. Mao, X. Huang, Z. Wang, B. Hua, Y. Liu, F. Zhang, Z. He, O. Jacobson, C. Gao, W. Wang, C. Yu, X. Zhu, F. Huang and X. Chen, *J. Am. Chem. Soc.*, 2018, **140**, 8005–8019; (*c*) G. Yu, Z. Yang, X. Fu, B. C. Yung, J. Yang, Z. Mao, L. Shao, B. Hua, Y. Liu, F. Zhang, Q. Fan, S. Wang, O. Jacobson, A. Jin, C. Gao, X. Tang, F. Huang and X. Chen, *Nat. Commun.*, 2018, **9**, 766; (*d*) J. Zhou, Y. Zhang, G. Yu, M. R. Crawley, C. R. P. Fulong, A. E. Friedman, S. Sengupta, J. Sun, Q. Li, F. Huang and T. R. Cook, *J. Am. Chem. Soc.*, 2018, **140**, 7730–7736; (*e*) F. Danhier, O. Feron and V. Préat, *J. Controlled Release*, 2010, **148**, 135–146; (*f*) K. Greish, in *Cancer Nanotechnology: Methods and Protocols*, ed. S. R. Grobmyer and B. M. Moudgil, Humana Press, Totowa, NJ, 2010, pp. 25–37.
8 (*a*) N. Graf and S. J. Lippard, *Adv. Drug Delivery Rev.*, 2012, **64**, 993–1004; (*b*) K. Lemma, A. M. Sargeson and L. I. Elding, *J. Chem. Soc., Dalton Trans.*, 2000, 1167–1172.
9 R. O. Williams Iii, V. Mahaguna and M. Sriwongjanya, *Eur. J. Pharm. Biopharm.*, 1998, **46**, 355–360.
10 (*a*) A. E. Pegg, *J. Biol. Chem.*, 2016, **291**, 14904–14912; (*b*) T. R. Murray-Stewart, P. M. Woster and R. A. Casero, *Biochem. J.*, 2016, **473**, 2937–2953.
11 (*a*) R. A. Casero, Jr. and L. J. Marton, *Nat. Rev. Drug Discovery*, 2007, **6**, 373–390; (*b*) A. J. Palmer and H. M. Wallace, *Amino Acids*, 2010, **38**, 415–422.
12 J. M. Woynarowski, W. G. Chapman, C. Napier, M. C. S. Herzig and P. Juniewicz, *Mol. Pharmacol.*, 1998, **54**, 770–777.
13 (*a*) S. S. S. Beevi, A. M. H. Rasheed and A. Geetha, *Jpn. J. Clin. Oncol.*, 2004, **34**, 379–385; (*b*) A. I. Fiaschi, A. Cozzolino, G. Ruggiero and G. A. Giorgi, *Eur. Rev. Med. Pharmacol. Sci.*, 2005, **9**, 361–367.